Deep Constrained Least Squares for Blind Image Super-Resolution
– Supplementary Material –

Ziwei Luo [1] Haibin Huang [2] Lei Yu [1] Youwei Li [1] Haoqiang Fan [1] Shuaicheng Liu [3,1*]
[1] Megvii Technology [2] Kuaishou Technology
[3] University of Electronic Science and Technology of China

I. More About DCLS Deconvolution

In this section, we provide additional analysis of the deep constrained least squares (DCLS) deconvolution module. Recall the reformulated degradation model in our paper:

$$\mathbf{y} = \mathbf{x}_{\downarrow_s} * \mathbf{k}_l + \mathbf{n}. \tag{1}$$

Note that this degradation model involves a deblurring problem on the downsampled image $\mathbf{x}_{\downarrow_s}$. Our work deals with it by incorporating the DCLS deconvolution module in the feature space and choosing to predict smooth filters for each channel through a CNN network (details are shown in Fig. 1). Compared with our DCLS, traditional constrained least squares (CLS) deconvolution is applied to RGB space and the smooth filter of CLS is fixed to be a Laplacian, given by

$$\mathbf{P} = \begin{bmatrix} 0 & 1 & 0 \\ 1 & -4 & 1 \\ 0 & 1 & 0 \end{bmatrix}. \tag{2}$$

Feature space deconvolution. Our paper (Table 5 in the manuscript) has demonstrated that DCLS is better than CLS as well as another traditional deblurring method Wiener deconvolution in the RGB space.

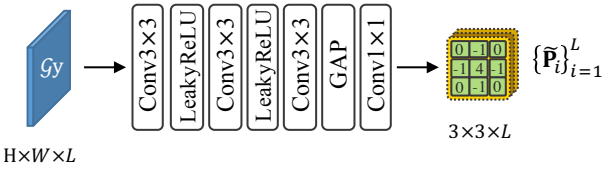

Figure 1. Architecture of the smooth filters predicting network. $\mathcal{G}\mathbf{y}$ is the primitive feature with size of $H \times W \times L$, where L is the number of channels. GAP denotes the global average pooling.

Effectiveness of reformulating degradation kernel. The proposed DCLS is based on Eq. (1) that is derived from classical degradation model with a high-resolution space kernel $\mathbf{k}_h$. To illustrate the effectiveness of using Eq. (1), we provide an experiment of substituting $\mathbf{k}_l$ with the primitive $\mathbf{k}_h$ in DCLS deconvolution and retrain that model on anisotropic Gaussian kernels. The result is shown in Table 1. Obviously, the high-resolution space kernel $\mathbf{k}_h$ is not compatible with the DCLS deconvolution module. Using reformulated kernel $\mathbf{k}_l$ can obtain an improvement of 0.67dB in PSNR. We also show more examples of the reformulated kernels in Fig. 2.

Method	PSNR	SSIM
DCLS with $\mathbf{k}_l$	28.99	0.7964
DCLS with $\mathbf{k}_h$	28.32	0.7762

Table 1. Quantitative results of substituting low-resolution space kernel $\mathbf{k}_l$ with high-resolution space kernel $\mathbf{k}_h$ in the DCLS deconvolution.

II. Analysis of the Computational Cost

Since we incorporate the dynamic deep linear kernel module which uses multi-layer filters and the dual-path network which uses additional convolutions to process the primitive features, the number of parameters of our method is subsequently increased. As shown in Table 2. However, we also find that adopting the dynamic deep linear kernel allows us to handle blind SR without additional iteration, thus our method requires fewer computational costs and performs slightly faster.

Method	#Params	FLOPs	Time
IKC [2]	5.29M	2178.72G	0.488s
DANv1 [5]	4.33M	926.72G	0.087s
DANv2 [6]	4.71M	918.12G	0.072s
DCLS	9.22M	368.15G	0.068s

Table 2. Comparison of model parameters, FLOPs, and inference time. '#Params' means number of parameters. The FLOPs are calculated with input size of 270×180.

*Corresponding author.

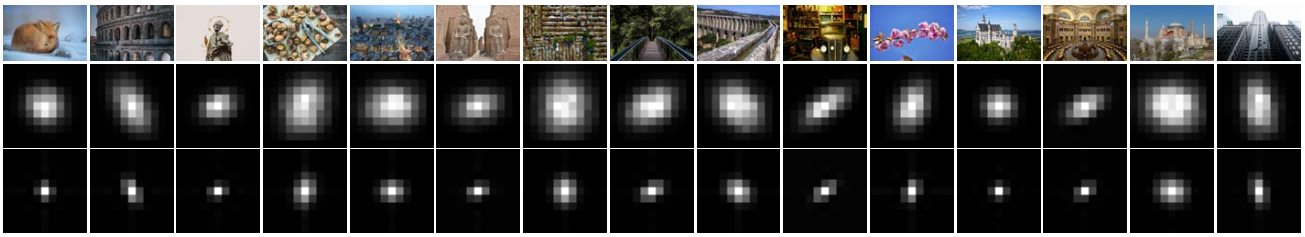

Figure 2. Visual examples of reformulated kernels. The top row and middle row are the LR images and the corresponding primitive kernels from DIV2KRK. The bottom row is reformulated kernels.

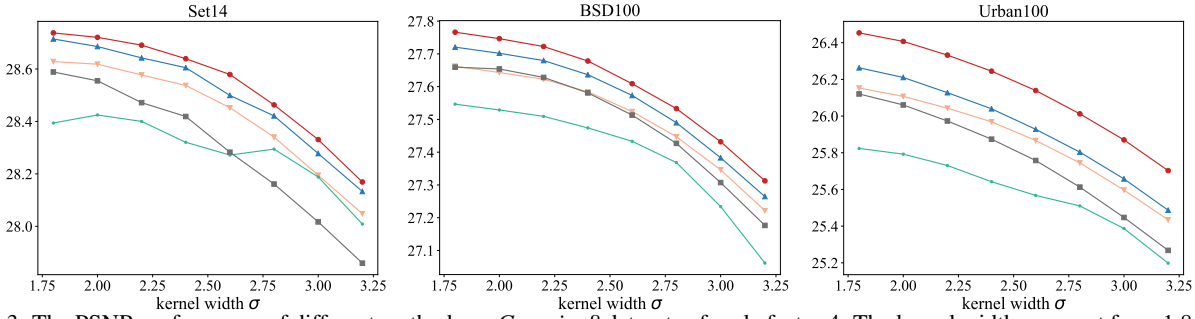

Figure 3. The PSNR performance of different methods on *Gaussian8* datasets of scale factor 4. The kernel width σ are set from 1.8 to 3.2.

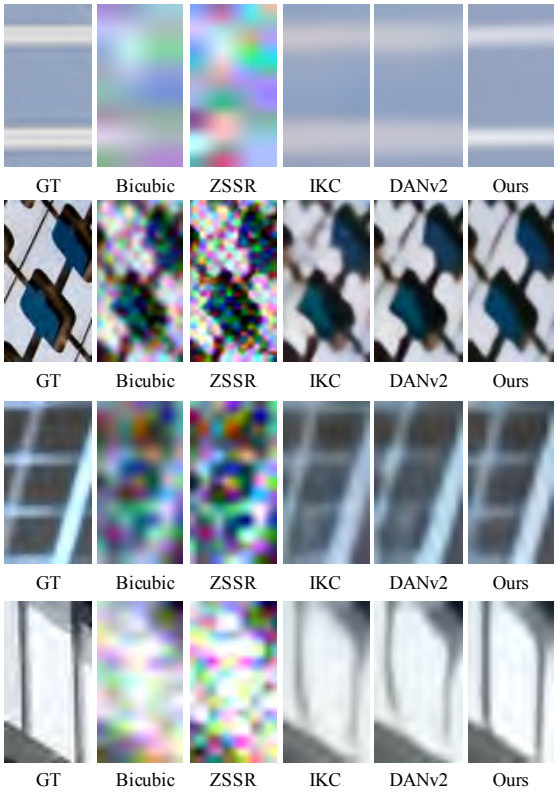

Figure 4. Visual results of *Img 33, Img 41, Img 44, Img52* from noisy Urban100.

III. Additional Results

Gaussian8. We provide more visual comparison results among the proposed DCLS and other state-of-the-art blind SR methods, including ZSSR [7], CARN [1], IKC [2], DANv2 [6] and AdaTarget [3], on *Gaussian8* kernels, as shown in Fig. 5 and Fig. 6. In addition, we give the results of SR evaluation on different kernel widths as illustrated in Fig. 3. These results demonstrate that our method achieves the best performance on isotropic Gaussian kernels. Fig. 4 shows more results on noisy dataset, which further demonstrate the superiority of our method.

DIV2KRK. We also provide more comparison results (including ZSSR [7], IKC [2], DANv2 [6], AdaTarget [3] and KOALAnet [4]) on DIV2KRK [2] to show the superiority of the proposed method, as illustrated in Fig. 7 and Fig. 8.

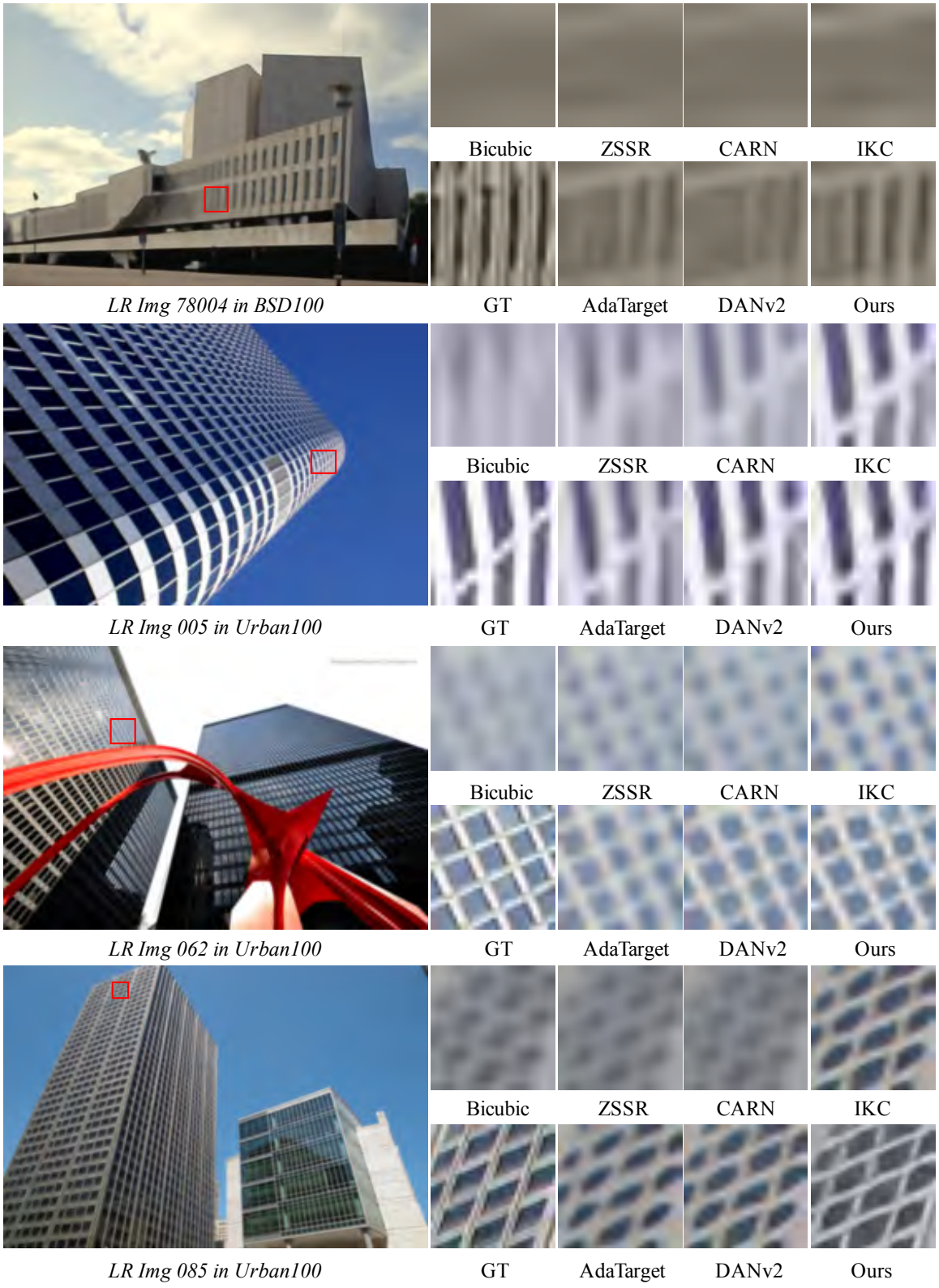

Figure 5. Visual comparison of different methods on *Gaussian8* kernels for scale factor 4.

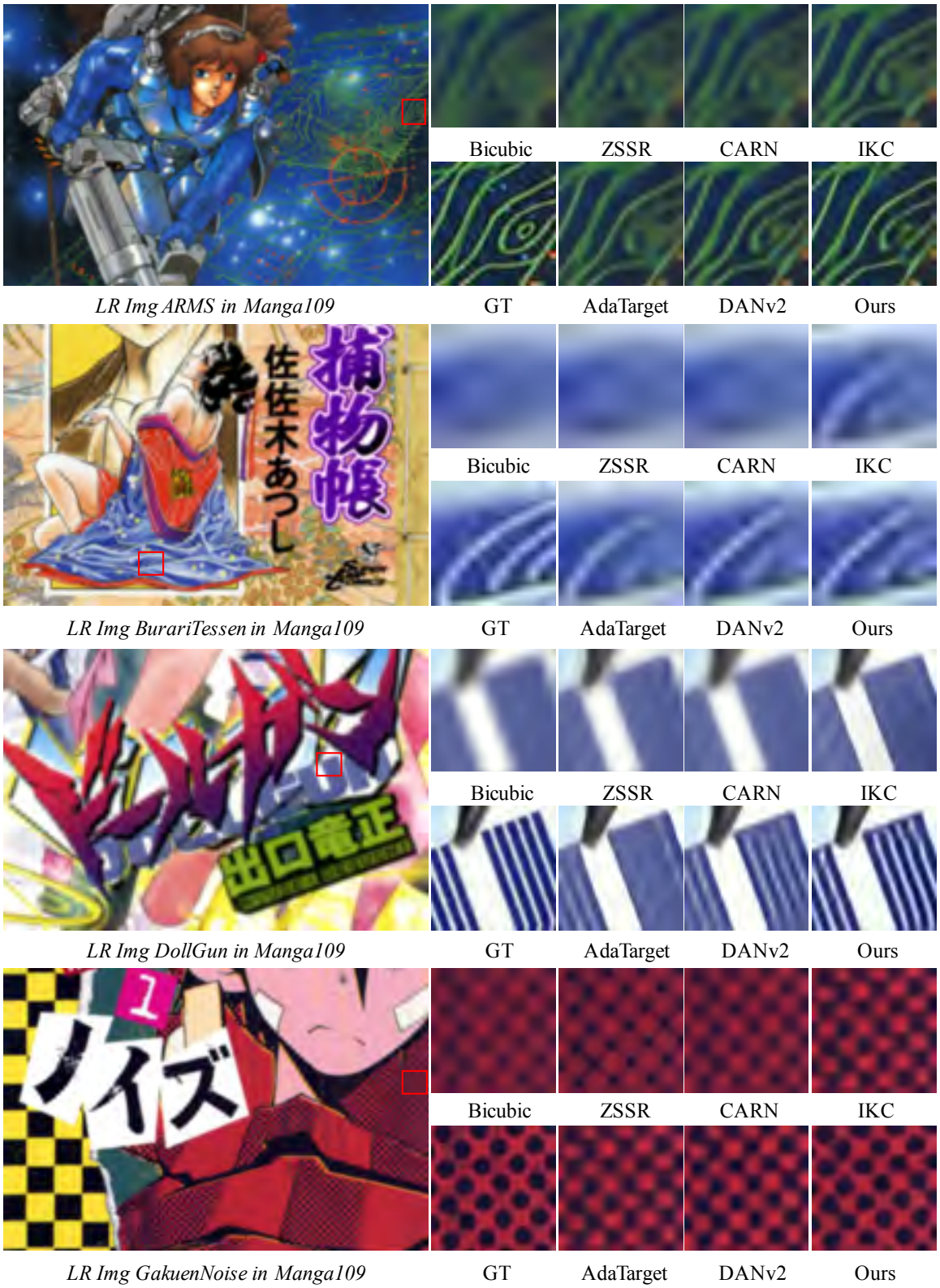

Figure 6. Visual comparison of different methods on *Gaussian8* kernels for scale factor 4.

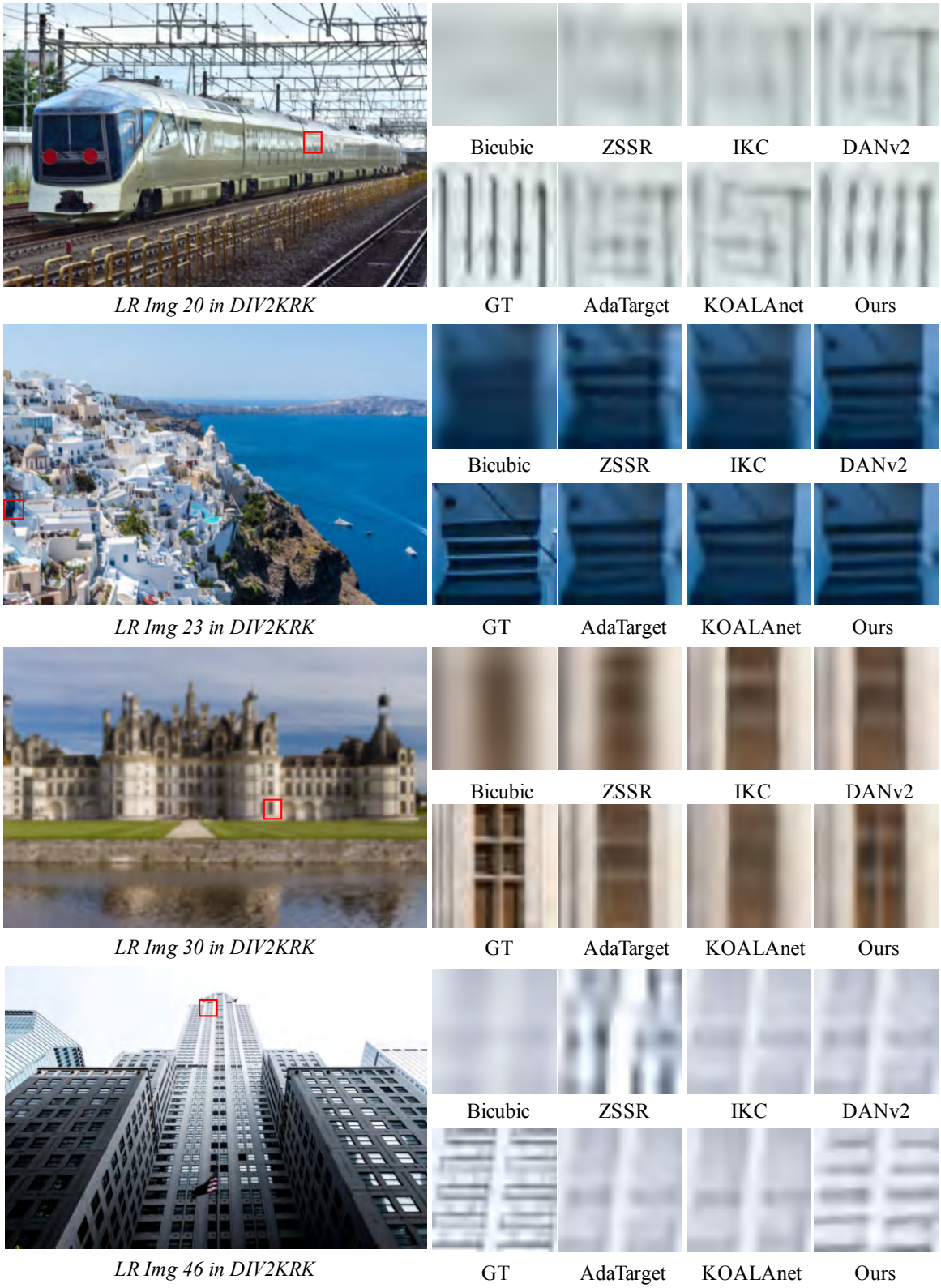

Figure 7. Visual comparison of different methods on DIV2KRK [2] dataset for scale factor 4.

Figure 8. Visual comparison of different methods on DIV2KRK [2] dataset for scale factor 4.

References

[1] Namhyuk Ahn, Byungkon Kang, and Kyung-Ah Sohn. Fast, accurate, and lightweight super-resolution with cascading residual network. In *Proc. ECCV*, pages 252–268, 2018. 2

[2] Jinjin Gu, Hannan Lu, Wangmeng Zuo, and Chao Dong. Blind super-resolution with iterative kernel correction. In *Proc. CVPR*, pages 1604–1613, 2019. 1, 2, 5, 6

[3] Younghyun Jo, Seoung Wug Oh, Peter Vajda, and Seon Joo Kim. Tackling the ill-posedness of super-resolution through adaptive target generation. In *Proc. CVPR*, pages 16236–16245, 2021. 2

[4] Soo Ye Kim, Hyeonjun Sim, and Munchurl Kim. Koalanet: Blind super-resolution using kernel-oriented adaptive local adjustment. In *Proc. CVPR*, pages 10611–10620, 2021. 2

[5] Zhengxiong Luo, Yan Huang, Shang Li, Liang Wang, and Tieniu Tan. Unfolding the alternating optimization for blind super resolution. In *Proc. NeurIPS*, 2020. 1

[6] Zhengxiong Luo, Yan Huang, Shang Li, Liang Wang, and Tieniu Tan. End-to-end alternating optimization for blind super resolution. *arXiv preprint arXiv:2105.06878*, 2021. 1, 2

[7] Assaf Shocher, Nadav Cohen, and Michal Irani. "zero-shot" super-resolution using deep internal learning. In *Proc. CVPR*, pages 3118–3126, 2018. 2